

# One-dimensional ice in bikitaite: single-crystal X-ray diffraction, infra-red spectroscopy and ab-initio molecular dynamics studies

Simona Quartieri <sup>a,\*</sup>, A. Sani <sup>a</sup>, G. Vezzalini <sup>a</sup>, E. Galli <sup>a</sup>, E. Fois <sup>b</sup>, A. Gamba <sup>b</sup>,  
G. Tabacchi <sup>b</sup>

<sup>a</sup> Dipartimento di Scienze della Terra, Università di Modena, via S. Eufemia 19, 41100 Modena, Italy

<sup>b</sup> Istituto di Scienze Matematiche, Fisiche e Chimiche, Università dell'Insubria, Sede di Como, Via Lucini 3, 22100 Como, Italy

## Abstract

The crystal structure of bikitaite,  $\text{Li}_2[\text{Al}_2\text{Si}_4\text{O}_{12}] \cdot 2\text{H}_2\text{O}$ , from North Carolina (USA) is triclinic, space group  $P1$ , with  $a=8.6146(6)$  Å,  $b=4.9570(5)$  Å,  $c=7.6032(6)$  Å,  $\alpha=89.899(8)^\circ$ ,  $\beta=114.394(5)^\circ$ ,  $\gamma=89.934(7)^\circ$ . The structure was refined using 8225 reflections, in the angular range  $5 < 2\theta < 84^\circ$ , and yielded an  $R_w=3.02\%$ . The average T–O distances and the ‘average long-range order coefficient’  $S$  calculated for the framework tetrahedral sites indicates an almost complete (Si, Al) ordering, similar to that found for bikitaite from Bikita (Zimbabwe) [G. Bissert, F.N. Liebau, Jb. Miner. Mh. H 6 (1986) 241] and in contrast to the partially or completely disordered structures refined in the space groups  $P1$  and  $P2_1$  on samples from the same locality [K. Ståhl, Å. Kvik, S. Ghose, Zeolites 9 (1989) 303; V. Kocman, R. Gait, J. Rucklidge, Am. Mineral. 59 (1974) 71]. In parallel, a series of ab-initio molecular dynamics simulations was performed on systems with the stoichiometry and the cell parameters of bikitaite from North Carolina, but with various (Si, Al) distributions. The micro-IR spectrum of bikitaite is also reported and compared with the simulated vibrational bands. Both experimental and simulation results are consistent with the literature data and confirm the presence of a stable one-dimensional chain of hydrogen-bonded water molecules. The presence and the stability of this ‘one-dimensional ice’ is independent of the (Si, Al) distribution in the framework. © 1999 Elsevier Science B.V. All rights reserved.

**Keywords:** Ab-initio molecular dynamics; Bikitaite zeolite crystal structure; FTIR microscopy; One-dimensional water chains; (Si, Al) ordering

## 1. Introduction

Bikitaite,  $\text{Li}_2[\text{Al}_2\text{Si}_4\text{O}_{12}] \cdot 2\text{H}_2\text{O}$ , is a rare zeolite found for the first time at Bikita, Zimbabwe [4] and then at King’s Mountain, North Carolina, USA [5]. The structure can be described by sheets of six-membered rings of T(1) and T(3) tetrahedra, connected by zig-zag chains of T(2) tetrahe-

dra. The framework is characterized by the presence of a one-dimensional channels system. These eight-ring straight channels, running along  $b$ , contain  $\text{Li}^+$  cations and water molecules. These water molecules form chains (one per channel) held together by hydrogen bonds. Each  $\text{Li}^+$  is four-coordinated by three framework oxygen atoms and one water oxygen [Fig. 1(a) and (b)].

The topological symmetry of bikitaite  $Cmcm$  is lowered to  $P2_1$  or  $P1$  by the distribution of the  $\text{Li}^+$  cations on the extraframework sites and by

\* Corresponding author. Fax: +39-059-417-399.  
E-mail address: quartieri@unimo.it (S. Quartieri)

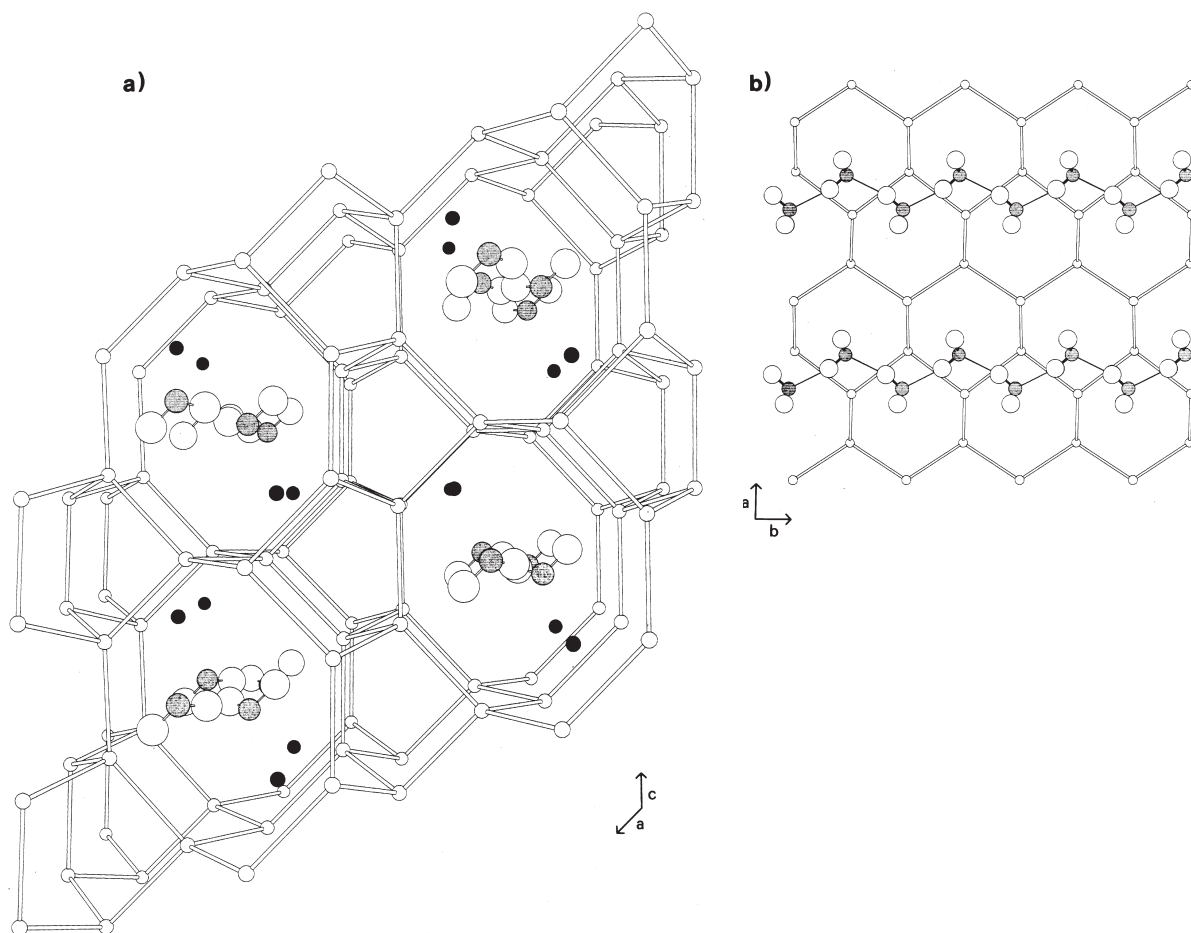


Fig. 1. Schematic representation of the structure of bikitaite. Tetrahedral cations as small open circles, water oxygen atoms in grey, lithium atoms in black, and hydrogen atoms as open circles. (a) Perspective view along  $b$ . (b) Projection on the  $XY$  plane.

the (Si, Al) ordering. In particular, a completely disordered (Si, Al) distribution on the tetrahedral sites forming the six-ring sheets (T1 and T3) is consistent with the space group  $P2_1$ , whereas the complete ordering further lowers the symmetry to  $P1$ .

Two X-ray [1,3] and one neutron [2] diffraction studies are reported for bikitaite from type locality (Bikita) and different space groups were determined, depending on the (Si, Al) ordering degree present in the crystals. In particular, bikitaite refined by Kocman et al. [3] is characterized by a completely disordered (Si, Al) distribution in the six-ring sheets — and by a consequent space group

$P2_1$  — whereas Bissert and Liebau [1] refined an almost completely ordered sample in the space group  $P1$ .

Notwithstanding the different space groups and (Si, Al) distribution in the framework sites, all these bikitaite samples exhibit the peculiar one-dimensional chain of hydrogen-bonded water molecules in the channels system. It is hence interesting to examine the following items:

1. the actual space group and (Si, Al) distribution of bikitaite from North Carolina, in comparison with the samples from Bikita, by means of an accurate single-crystal X-ray diffraction study;
2. the dynamical properties of the water molecules

chain and the possible influence of the (Si, Al) distribution on its stability by means of ab-initio molecular dynamics (MD) simulations on systems with different (Si, Al) distributions.

Moreover, the experimental micro-IR spectrum of bikitaite (up to now not reported in literature) and the simulations of the vibrational properties are discussed.

## 2. Methods

### 2.1. X-ray data collection and structure refinement

X-ray diffraction data collection was carried out on a Siemens four-circle diffractometer using a rotating anode generator. 8270 reflections over the range  $5 < 2\theta < 84^\circ$  were collected in the triclinic space group *P1*, out of which 8225 with  $I > 3\sigma(I)$  were used in the structure refinement. After comparison between the intensities  $hkl$  and  $h\bar{k}l$ , the structure refinement was performed in the space group *P1*. The intensity values were corrected for Lorentz-polarization and absorption. The correc-

tion for absorption was made by the semi-empirical method proposed by North et al. [6].

Structure refinement was done by full-matrix least squares analysis with the program SHELX76 [7], starting from positional parameters by Ståhl et al. [2] and considering all atoms as neutral. A structure refinement performed using the ionic lithium scattering curve did not furnish significantly different results in either position or occupancy parameters. The positions of all hydrogen atoms were localized by Fourier map analysis. At the end of the last anisotropic refinement cycle, the *R* and *R<sub>w</sub>* indices were 2.78% and 3.02% respectively. Details on data collection, cell parameters and structure refinement are given in Table 1. The final atomic coordinates are reported in Table 2. Tables 3 and 4 give the bond distances and angles for the framework and extraframework atoms respectively. A copy of the table of observed

Table 1  
Details of the X-ray data collection and structural refinement

Cell parameters	
<i>a</i> (Å)	8.6146(6)
<i>b</i> (Å)	4.9570(5)
<i>c</i> (Å)	7.6032(6)
$\alpha$ (deg)	89.899(8)
$\beta$ (deg)	114.394(5)
$\gamma$ (deg)	89.934(7)
<i>V</i> (Å <sup>3</sup> )	295.69
Space group	<i>P1</i>
Crystal size (mm <sup>3</sup> )	0.05 × 0.14 × 0.20
Instrument	Siemens rotating anode (52 kV × 100 mA)
Radiation, wavelength (Å)	Mo K $\alpha$ , 0.710 69
2 $\theta$ interval (deg)	5– 84
$\omega$ scan with $\Delta\omega$ (deg)	1
<i>R<sub>int</sub></i> of Friedel pairs	0.017
No. of reflections measured	8270
No. of reflections with $I > 3\sigma(I)$ used in the refinement	8212
<i>R</i> (%)	2.78
<i>R<sub>w</sub></i> (%)	3.02

Table 2  
Atomic coordinates and *B<sub>eq</sub>* of bikitaite from North Carolina. Atom labels are from Ref. [2]

Atom	<i>x/a</i>	<i>y/b</i>	<i>z/c</i>	<i>B<sub>eq</sub></i> (Å <sup>2</sup> )
Si11	0.107 13(6)	0.864 55(9)	0.099 43(6)	0.46
Si12	0.1038	0.8006	0.5049	0.53
Al13	0.380 55(6)	0.874 28(9)	0.939 22(7)	0.53
Al21	0.900 48(6)	0.364 69(9)	0.908 73(7)	0.57
Si22	0.892 20(5)	0.299 31(8)	0.487 93(6)	0.53
Si23	0.619 75(6)	0.374 90(9)	0.065 01(6)	0.42
O11	0.2639(1)	0.7395(2)	0.0610(2)	0.74
O12	0.0863(1)	0.1822(2)	0.0454(1)	0.80
O13	0.1590(2)	0.8283(3)	0.3272(1)	1.39
O14	0.0543(1)	0.4865(2)	0.5139(2)	1.30
O15	0.2602(1)	0.8927(2)	0.6937(1)	1.25
O16	0.4524(1)	0.1970(2)	0.0306(1)	0.77
O21	0.7313(1)	0.2435(2)	0.9593(1)	0.74
O22	0.9317(1)	0.7052(2)	0.9754(1)	0.81
O23	0.8420(2)	0.3286(3)	0.6652(2)	1.45
O24	0.9376(1)	0.9877(2)	0.4633(2)	1.24
O25	0.7317(1)	0.3940(2)	0.2959(1)	1.18
O26	0.5619(1)	0.6771(2)	0.9841(1)	0.75
Li1	0.3115(4)	0.3640(6)	0.1506(5)	1.28
Li2	0.7018(4)	0.8678(5)	0.8796(5)	1.22
O17	0.4101(2)	0.3225(3)	0.4393(2)	2.18
H11	0.337(4)	0.301(8)	0.439(5)	5.91
H12	0.471(6)	0.184(9)	0.450(8)	5.76
O27	0.6002(2)	0.8213(3)	0.5927(2)	2.23
H21	0.661(6)	0.804(9)	0.537(6)	9.91
H22	0.503(4)	0.705(7)	0.552(5)	7.55

Table 3

Interatomic distances (Å) and angles (deg) for the framework atoms from the X-ray structure refinement (standard deviations in parentheses)

Si11–O11	1.618(1)	Si12–O13	1.612(1)	Si22–O14	1.620(1)
Si11–O12	1.618(1)	Si12–O14	1.624(1)	Si22–O23	1.583(1)
Si11–O13	1.610(1)	Si12–O15	1.578(1)	Si22–O24	1.623(1)
Si11–O22	1.620(1)	Si12–O24	1.622(1)	Si22–O25	1.610(1)
Si23–O16	1.618(1)	Al13–O11	1.755(1)	Al21–O12	1.755(1)
Si23–O21	1.622(1)	Al13–O15	1.723(1)	Al21–O21	1.760(1)
Si23–O25	1.620(1)	Al13–O16	1.754(1)	Al21–O22	1.752(1)
Si23–O26	1.616(1)	Al13–O26	1.751(1)	Al21–O23	1.716(1)
Si11–O11–Al13	130.70(6)			Si23–O21–Al21	133.18(6)
Si11–O12–Al21	128.92(6)			Si11–O22–Al21	129.44(6)
Si11–O13–Si12	149.8(1)			Si22–O23–Al21	150.1(1)
Si12–O14–Si22	140.66(6)			Si12–O24–Si22	139.08(6)
Si12–O15–Al13	151.22(6)			Si22–O25–Si23	150.36(6)
Si23–O16–Al13	135.09(6)			Si23–O26–Al13	134.39(6)
O11–Si11–O12	109.85(5)	O13–Si12–O14	106.82(7)	O14–Si22–O23	111.57(8)
O11–Si11–O13	105.75(7)	O13–Si12–O15	107.55(6)	O14–Si22–O24	108.88(5)
O11–Si11–O22	110.80(5)	O13–Si12–O24	109.29(7)	O14–Si22–O25	108.59(6)
O12–Si11–O13	109.39(6)	O14–Si12–O15	112.46(6)	O23–Si22–O24	110.50(8)
O12–Si11–O22	110.46(5)	O14–Si12–O24	109.22(4)	O23–Si22–O25	108.12(7)
O13–Si11–O22	110.49(7)	O15–Si12–O24	111.35(5)	O24–Si22–O25	109.14(6)
O16–Si23–O21	111.78(5)	O11–Al13–O15	111.79(4)	O12–Al21–O21	109.29(5)
O16–Si23–O25	107.49(5)	O11–Al13–O16	108.88(5)	O12–Al21–O22	109.28(5)
O16–Si23–O26	109.28(5)	O11–Al13–O26	110.14(5)	O12–Al21–O23	111.94(6)
O21–Si23–O25	110.62(5)	O15–Al13–O16	109.83(5)	O21–Al21–O22	107.97(5)
O21–Si23–O26	109.63(5)	O15–Al13–O26	109.17(4)	O21–Al21–O23	107.38(6)
O25–Si23–O26	107.94(5)	O16–Al13–O26	106.90(5)	O22–Al21–O23	110.88(6)

Table 4

Interatomic distances (Å) and angles (deg) for the extraframework atoms from the X-ray structure refinement<sup>a</sup> (standard deviations in parentheses)

Li1–O11	1.965(3)	Li2–O21	1.944(3)
Li1–O12	1.985(3)	Li2–O22	1.977(3)
Li1–O16	1.976(3)	Li2–O26	1.941(3)
Li1–O17	2.010(4)	Li2–O27	2.001(4)
O11–Li1–O12	105.2(2)	O21–Li2–O22	107.0(2)
O11–Li1–O16	108.5(2)	O21–Li2–O26	111.3(2)
O11–Li1–O17	114.0(2)	O21–Li2–O27	113.3(2)
O12–Li1–O16	107.9(2)	O22–Li2–O26	110.4(1)
O12–Li1–O17	107.2(2)	O22–Li2–O27	105.9(2)
O16–Li1–O17	113.5(2)	O26–Li2–O27	108.9(2)
O17–H11	0.90(3)	O27–H21	0.80(4)
O17–H12	0.85(5)	O27–H22	0.96(3)
O17–H22	2.10(3)	O27–H12	2.15(5)
O17–O27	2.932(2)	O27–O17	2.935(2)

<sup>a</sup> The water molecule bond angles are not reported owing to the very high standard deviations.

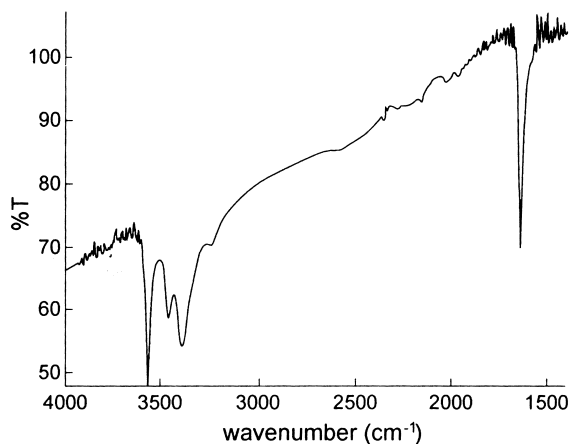


Fig. 2. Micro-IR spectrum of bikitaite from North Carolina.

and calculated structure factors and of the anisotropic temperature factors may be obtained by the authors.

## 2.2. Microanalysis and IR spectroscopy

The chemical analysis of the sample under study was performed using an electron microprobe in the wavelength-dispersive mode on an ARL-SEMQ instrument, operated at 15 kV, 20 nA beam current and with a defocused beam (spot size 20  $\mu\text{m}$ ). The results of the chemical analysis confirm the chemical composition reported by Leavens et al. [5] for bikitaite from North Carolina.

The micro-IR spectrum of bikitaite from North Carolina was recorded by means of a Perkin Elmer Spectrum 2000 FTIR microscope (Fig. 2). Owing to the extreme paucity of the available material, we worked on single crystal. The small and thin crystal slabs necessary for the micro-IR analysis were obtained by applying an oriented pressure on a larger crystal. Notwithstanding this, the bands corresponding to the framework atom modes (around 1100  $\text{cm}^{-1}$ ) were saturated and so they are not reported in Fig. 2.

## 2.3. Calculations

We used the first-principles MD technique due to Car and Parrinello [8,9]. This method has been employed in a wide range of applications and it is particularly suited for exploring, with ab-initio-level accuracy, the finite-temperature behaviour of large systems [10,11]. This approach owes its success to the accurate treatment of the interatomic forces that, unlike conventional MD, are calculated from the electronic structure corresponding to each instantaneous ionic configuration. According to this methodology, the dynamics is derived from a classical Lagrangian, which includes the ionic degrees of freedom (nuclear positions and velocities), extended with a fictitious system that includes the electronic degrees of freedom (wavefunction coefficients and their time derivative). The equations of motion are integrated using standard finite difference techniques. The electronic structure problem is solved by the density functional formalism [12].

We adopted a supercell (from here on MD-cell) consisting of two crystallographic cells along *b* (the direction of the water chains)  $[\text{Li}_2(\text{Al}_2\text{Si}_4\text{O}_{12}) \cdot 2\text{H}_2\text{O}]_2$ , with the cell parameters determined experimentally for bikitaite from North

Carolina and periodic boundary conditions. Norm-conserving pseudopotentials were used to model the ions–electrons interactions [13,14]: d-nonlocality was adopted for Al, Si, and O atoms, p-nonlocality for Li atoms and a local norm-conserving pseudopotential was used for H. Orbitals were expanded in plane waves up to a cutoff of 60 Ry; electron–electron interactions were calculated with a gradient corrected density functional approximation [15,16]. The equations of motion were integrated using a time step of 0.121 fs and a fictitious mass of 500 au was used for the wavefunction coefficients [8,10].

Four structures with different (Si, Al) ordering were studied at 298 K. A long trajectory (**a**) (4 ps of elapsed time) was performed for an ordered structure with 100% Al in both Al13 and Al21 positions (labels as in Table 2), in order to obtain a detailed vibrational spectrum. Other shorter trajectories (about 1 ps) were performed with different (Si, Al) ordering: (**b**) a partially disordered structure, obtained by setting in one half MD-cell an Si atom in the Al21 site and an Al atom in the Si22 site; (**c**) an ordered structure obtained by inverting Al and Si positions in the hexagonal six-ring sheets; (**d**) a structure with half an MD-cell like (**a**) and half MD-cell like (**c**).

Structure (**d**) violates the Löwenstein rule, but it was the only way to simulate partial disorder in the Al13 and Al21 sites while maintaining the same number of atoms and the MD-cell of the other simulated structures. Concerning the (Si, Al) distribution used in simulation (**b**), no explanation has been given up to now about its absence among the natural bikitaite, notwithstanding it does not violate the Löwenstein rule. This last point will be discussed below.

A more detailed description of the theoretical method and of the simulations is reported in Ref. [17].

## 3. Results and discussion

### 3.1. Diffraction results and comparison with the other bikitaite refinements

The triclinic crystal structure of bikitaite from North Carolina is extremely similar in the atomic

positions to that determined by Bissert and Liebau [1] and scarcely deviates from that of Ståhl et al. [2]. The location of the water hydrogen atoms succeeded — even if with rather high standard deviations, especially on the bond angles — and the positions are in good agreement with those determined by neutron diffraction [2]; as previously found for the other bikitaite samples, the water molecules form infinite hydrogen-bonded chains, are coordinated only to  $\text{Li}^+$  cations and no hydrogen bonds with the framework oxygen atoms are present. Our theoretical and experimental results indicate that water molecules show a behaviour typical of a solid, as they do not diffuse along the bikitaite channels. Their only motions are oscillations around their crystallographic positions. These one-dimensional water chains, which therefore could be called ‘one-dimensional ice’, deserve great attention, considering the present technological interest for low-dimensionality systems.

Significant differences among bikitaite from North Carolina and the other bikitaite samples were detected in the framework (Si, Al) distribution. Average T–O distances of 1.616, 1.609, 1.609 and 1.619 Å for four of the six crystallographically independent tetrahedral sites and 1.746 Å for the other two suggest an almost completely ordered (Si, Al) distribution in bikitaite from North Carolina. Such a distribution was accurately evaluated by the method developed by Alberti and Gottardi [18] and compared with those calculated, with the same method, for the other bikitaite samples (Table 5). The ‘average long-range order coefficient’  $S$  calculated for the bikitaite sample studied here (0.90) is virtually identical to that obtained from the results of the Bissert and Liebau refinement (0.91) and significantly different from those values obtained by the Ståhl et al. (0.69) and Kocman et al. (0.42) refinements [19].

These values indicate that the degree of (Si, Al) ordering in bikitaite from North Carolina and in that refined by Bissert and Liebau [1] is significantly higher than that of bikitaite samples refined by Ståhl et al. [2] and, especially, by Kocman et al. [3]. In particular, almost only Si is located in the tetrahedral sites Si12 and Si22 — forming a zig-zag chain connecting the six-ring sheets — whereas

Table 5

Mean T–O distances, percentage of Al in the tetrahedral sites and ‘long-range order coefficients’ for the bikitaite samples refined in the space group  $P1$

Site	Ref.	Mean T–O (Å)	Al content <sup>a</sup> (%)	$S$ <sup>b</sup>
Si11	[2]	1.635	13.1	0.59
	[1]	1.617	0.0	1.0
	this work	1.616	0.0	1.0
Si12	[2]	1.607	2.9	0.91
	[1]	1.608	1.4	0.96
	this work	1.609	2.0	0.94
Al13	[2]	1.725	77.8	–0.68
	[1]	1.743	89.7	–0.85
	this work	1.746	91.8	–0.88
Al21	[2]	1.725	75.8	–0.65
	[1]	1.747	90.0	–0.86
	this work	1.746	89.3	–0.84
Si22	[2]	1.609	4.0	0.87
	[1]	1.610	3.0	0.91
	this work	1.609	2.6	0.91
Si23	[2]	1.636	16.7	0.47
	[1]	1.618	4.4	0.86
	this work	1.619	5.1	0.84

<sup>a</sup> Ref. [18].

<sup>b</sup> ‘Long-range order coefficient’ after Ref. [19].

Si and Al strictly alternate in the sites forming the six-rings.

### 3.2. Vibrational properties of the one-dimensional ice

The region of the micro-IR spectrum between 1500 and 4000  $\text{cm}^{-1}$  displays  $\text{H}_2\text{O}$ -specific absorptions at 3578.8, 3471.4, 3400.8  $\text{cm}^{-1}$  (stretching modes) and 1640.8  $\text{cm}^{-1}$  (bending mode). A stretching zone at high frequency is characteristic of weak hydrogen bonds, with a distance between the donor and acceptor oxygen atoms larger than 2.7 Å [20]. These spectroscopic data are consistent with the interatomic distances derived by X-ray diffraction (Table 4) and by MD simulations (see Table 7 below). Moreover, the presence of well-defined O–H stretching bands at significantly different frequencies is consistent with the presence of a one-dimensional chain of hydrogen-bonded

water molecules, in which only one hydrogen per water molecule is involved.

The simulation of the vibrational properties of the water chains hosted in bikitaite was performed in the simulation system (a). The vibrational theoretical spectrum was obtained from the FT of the velocity autocorrelation function. The results are reported in Fig. 3(a) and (b) for the bending and stretching zone respectively.

Fig. 3a reports the bending zone of the calcu-

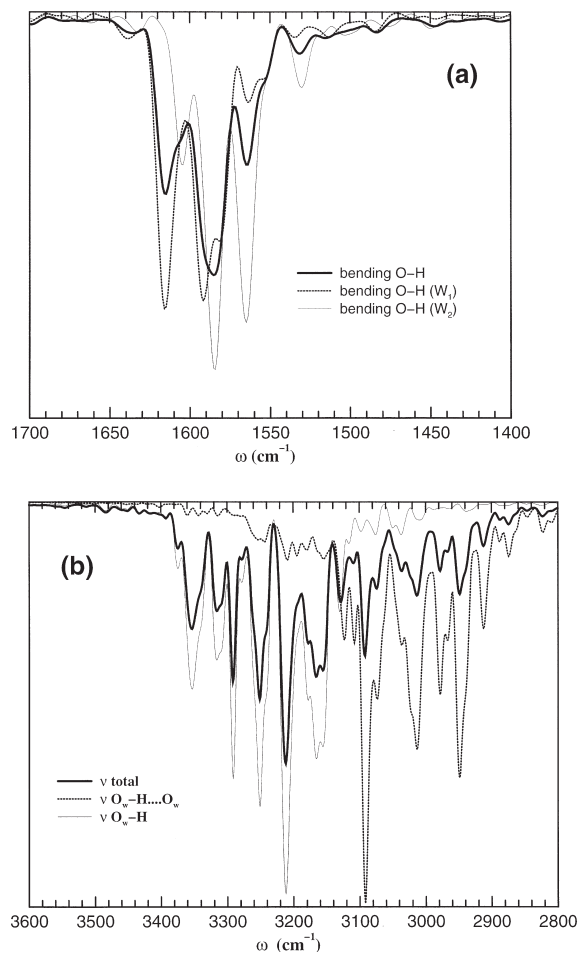


Fig. 3. Simulated vibrational spectra for structure (a). (a) H<sub>2</sub>O bending zone. Thick solid line: total spectrum; dashed line and thin solid lines: contributions of the two crystallographically independent water molecules. (b) O–H stretching zone. Thick solid line: total spectrum; dotted line: contribution of the bonds involved in the O–H...O bridges; thin solid line: contribution of the O–H bonds not involved in hydrogen bonds.

lated vibrational spectrum, along with the separated contributions of the two water molecules (corresponding to the oxygen atoms O17 and O27 of Table 2). These partial contributions were calculated from the FT of the autocorrelation functions of the interatomic bond angles of the two distinct water molecules. The positions of these two components are slightly different, in agreement with the presence in bikitaite channels of two crystallographically independent water molecules.

Fig. 3(b) reports the stretching zone of the calculated vibrational spectrum, along with the contributions of the four crystallographically independent intramolecular O–H bonds (labelled in Table 5 as O17–H11, O17–H12, O27–H21, O27–H22). The stretching band is broadened on a large region (about  $500 \text{ cm}^{-1}$ ) and its centre (at about  $3150 \text{ cm}^{-1}$ ) appears to be red-shifted with respect to the stretching frequencies calculated with the same approximations for an isolated water molecule ( $3354$  and  $3454 \text{ cm}^{-1}$ , for the symmetric and asymmetric stretching modes respectively). The calculated shift moves in agreement of that experimentally observed with respect to gas-phase water [21]. The discrepancy in the absolute values of the experimental and calculated vibrational frequencies mainly depends on the fictitious mass used in the Car–Parrinello MD simulations [22,23].

Within the broadened stretching band, we can distinguish two main components, both characterized by a complex fine structure. The one at lower frequencies is associated with the vibrations of O17–H11 and O27–H22 bonds, involved in the O–H...O bridges. The component at higher frequencies is ascribed to the stronger O–H bonds, not involved in hydrogen bonding interactions.

### 3.3. Effects of the (Si, Al) ordering

In Tables 6 and 7 we report the mean geometrical parameters calculated from MD trajectory (a), for the framework and the extraframework atoms respectively. These results are to be compared with the experimental data for bikitaite from North Carolina reported in Tables 3 and 4. The simulation–experiment agreement is satisfactory, even if the simulated bond length values are systematically a few hundredths of an ångström larger than the

Table 6

Interatomic distances (Å) and angles (deg) for the framework atoms from the MD simulation (a)

Si11–O11	1.638	Si12–O13	1.640	Si22–O14	1.651
Si11–O12	1.638	Si12–O14	1.647	Si22–O23	1.614
Si11–O13	1.647	Si12–O15	1.619	Si22–O24	1.646
Si11–O22	1.641	Si12–O24	1.647	Si22–O25	1.648
Si23–O16	1.637	Al13–O11	1.787	Al21–O12	1.796
Si23–O21	1.637	Al13–O15	1.780	Al21–O21	1.798
Si23–O25	1.662	Al13–O16	1.795	Al21–O22	1.792
Si23–O26	1.637	Al13–O26	1.784	Al21–O23	1.769
Si11–O11–Al13	127.62			Si23–O21–Al21	130.96
Si11–O12–Al21	125.22			Si11–O22–Al21	125.62
Si11–O13–Si12	141.11			Si22–O23–Al21	139.30
Si12–O14–Si22	138.25			Si12–O24–Si22	135.68
Si12–O15–Al13	138.16			Si22–O25–Si23	139.05
Si23–O16–Al13	130.78			Si23–O26–Al13	132.45
O11–Si11–O12	109.97	O13–Si12–O14	107.03	O14–Si22–O23	109.24
O11–Si11–O13	103.65	O13–Si12–O15	110.22	O14–Si22–O24	111.48
O11–Si11–O22	110.74	O13–Si12–O24	107.32	O14–Si22–O25	108.08
O12–Si11–O13	111.67	O14–Si12–O15	110.40	O23–Si22–O24	109.75
O12–Si11–O22	109.83	O14–Si12–O24	111.03	O23–Si22–O25	110.79
O13–Si11–O22	110.59	O15–Si12–O24	110.47	O24–Si22–O25	107.24
O16–Si23–O21	110.66	O11–Al13–O15	116.90	O12–Al21–O21	108.28
O16–Si23–O25	106.56	O11–Al13–O16	106.37	O12–Al21–O22	108.73
O16–Si23–O26	111.12	O11–Al13–O26	107.64	O12–Al21–O23	113.17
O21–Si23–O25	113.34	O15–Al13–O16	109.01	O21–Al21–O22	107.72
O21–Si23–O26	107.87	O15–Al13–O26	107.54	O21–Al21–O23	105.01
O25–Si23–O26	106.99	O16–Al13–O26	108.83	O22–Al21–O23	113.22

Table 7

Interatomic distances (Å) and angles (deg) for the extraframework atoms from the MD simulation (a)

Li1–O11	2.026	Li2–O21	2.006
Li1–O12	2.027	Li2–O22	2.008
Li1–O16	2.024	Li2–O26	1.987
Li1–O17	2.054	Li2–O27	2.051
O11–Li1–O12	101.51	O21–Li2–O22	103.44
O11–Li1–O16	103.44	O21–Li2–O26	106.81
O11–Li1–O17	121.56	O21–Li2–O27	120.09
O12–Li1–O16	105.10	O22–Li2–O26	109.26
O12–Li1–O17	109.90	O22–Li2–O27	108.03
O16–Li1–O17	112.15	O26–Li2–O27	107.53
O17–H11	0.992	O27–H21	0.982
O17–H12	0.998	O27–H22	1.000
O17–H22	1.872	O27–H12	1.900
O17–O27	2.831	O27–O17	2.831

experimental ones. This slight difference is, however, expected, since the experimental bond distances are determined from the centre of gravity

of the atomic positions derived by the structure refinement procedure, whereas the theoretical ones (Tables 6 and 7) are the averages of the bond distances calculated at each MD step. As an example, the Si11–O11 distance calculated along the MD simulation (a) from the average atomic position (1.631 Å) is closer to the corresponding experimental value (1.618 Å) than the bond distance reported in Table 6 (1.638 Å). Moreover, if we consider the Si12–O13 distance calculated from average positions (1.617 Å), our result is in quantitative agreement with the corresponding experimental one (1.612 Å).

The calculated data showing the largest deviations from experimental results are the hydrogen bond lengths (i.e. O27–H12 and O17–H22) and the distance between the two water molecules of the chain (i.e. –3% for O17–O27 separation). Such a result is typical of current density functional approximation when dealing with systems charac-

terized by weak bonds, such as the hydrogen bonds. However, the structural properties of the hydrogen-bonded water molecules chains are in fair agreement with the experimental ones.

For the sake of brevity, we do not report the geometrical parameters calculated from the other trajectories; however, they are consistent with the (Si, Al) distribution used in each simulation (e.g. T–O distances change according to the Al occupancy of T sites). It is worth noting that, independently from the (Si, Al) ordering adopted in the simulations, both the framework arrangement and the water chain are always stable, with the average water–water separation changing by a maximum of 1% in the four simulations. A similar variability (about 1%) is also observed in the water–water distance experimentally determined in the bikitaite structure refinements Refs. [1–3] (and this work).

We have calculated, for each simulation, the radial distribution functions (rdfs) for all the atomic species. Since  $\text{Li}^+$  showed large oscillations in its positions during the dynamics, we report in Fig. 4(a)–(d) the rdfs of  $\text{Li}^+$  from the framework atoms (O, Si, Al) and from the water oxygen atoms, calculated along the trajectory (a). From these plots it is clear that the simulated structure well resembles the experimental one.

Among the (Si, Al) distributions adopted in these MD simulations, the one assumed for simulation (b) is the only one never observed in nature for bikitaite. Hence, it is interesting to understand the reasons why Al atoms never enter the tetrahedral sites of the zig-zag chain (Si12 and Si22).

An indication comes from the inspection of the Li–O bond distances calculated along the four trajectories. In all the structures  $\text{Li}^+$  is coordinated to one water and three framework oxygen atoms, with an approximately tetrahedral coordination. However, in structure (b), three Li–O coordination distances (Li1–O12, Li2–O21, Li2–O22 in Table 7) become considerably longer (about 2.11 Å), with respect to the corresponding values obtained from the other two simulations and the structural refinement. This lengthening can be justified with the substitution of the Al of the six-ring coordinated to O12, O21 and O22, with an Si atom. On the contrary, the simultaneous substitution of Si

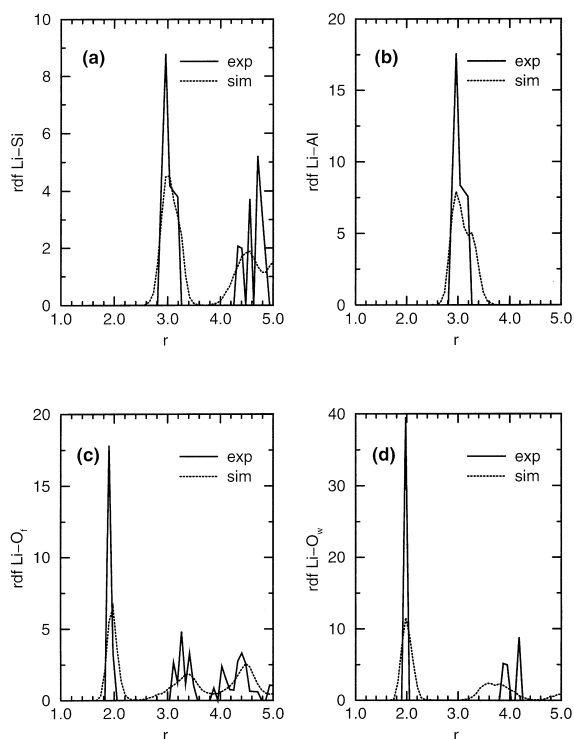


Fig. 4. Selected rdfs ( $r/\text{Å}$ ) for MD simulation (a): (a) Li–Si; (b) Li–Al; (c) Li– $\text{O}_{\text{frame}}$ ; (d) Li– $\text{O}_{\text{water}}$ .

for Al in the zig-zag chain does not affect the Li–O coordination distances.

Since the substitution of a trivalent Al for a tetravalent Si in framework sites — and the consequent Li–O bond lengthening — can influence the local charge balancing, we have calculated the bond strength [24] on the framework oxygen atoms for all the simulated and the refined bikitaite (see Table 8). As noted by Bissert and Liebau [1] for bikitaite from Bikita, also in the sample from North Carolina the framework oxygen atoms O15 and O23 are significantly undersaturated. From Table 8 we see that a similar undersaturation of only two framework oxygen atoms is also found in the simulations (a) and (c). On the contrary, the calculated structure (b) is characterized by a larger charge unbalancing, involving several framework oxygen atoms. This could be the main cause of the absence of this particular (Si, Al) distribution in natural bikitaite.

We can hence conclude that the results of this

Table 8  
Bond strength on the framework oxygen atoms for the refined and the simulated bikitaite structures

Framework oxygen	Structural refinement	MD simulations			
		(a)	(b)	(c)	(d)
O11	1.997	2.002	2.003	2.001	2.001
O12	1.995	1.999	2.104	2.000	2.003
O13	2.002	1.995	1.997	1.771	1.880
O14	1.984	1.993	1.883	1.995	1.992
O15	1.779	1.765	1.759	1.981	1.873
O16	1.998	2.001	2.008	2.010	2.006
O21	1.995	2.001	2.106	2.005	2.003
O22	1.994	1.999	2.107	2.001	1.999
O23	1.779	1.759	1.772	1.991	1.884
O24	1.983	1.996	1.874	1.990	1.992
O25	1.999	1.989	1.872	1.760	1.872
O26	2.002	2.008	2.011	2.002	2.001

experimental–theoretical investigation strengthen the hypothesis of Merlino [25] that the (Si, Al) distribution in bikitaite is always essentially ordered within each six-ring sheet (with Si and Al regularly alternating in the tetrahedral sites) and in the zig-zag chains (containing only Si atoms), whereas the ordering in adjacent sheets is not strictly correlated. Then, the different degrees of (Si, Al) disorder observed by Ståhl et al. [2] and Kocman et al. [3] could be due to the presence of antiphase domains in the structures.

#### 4. Conclusions

This work represents an example of a combined approach to the study of a zeolitic system, in which different experimental (single-crystal X-ray diffraction, micro-IR spectroscopy) and theoretical (ab-initio MD) techniques have been applied to achieve a deep description and structural interpretation of the system in study.

The following main results were obtained.

1. The triclinic crystal structure of bikitaite from North Carolina is extremely similar in atomic positions to that determined by Bissert and Liebau [1] and scarcely deviates from that of Ståhl et al. [2]. The (Si, Al) distribution is almost completely ordered, in agreement with

the results of Bissert and Liebau [1]. The location of the water hydrogen atoms succeeded and the positions are in good agreement with those determined by neutron diffraction [2]. Hence, for bikitaite from North Carolina the peculiar presence of a ‘one-dimensional ice’ running along the *b* direction is also confirmed.

2. In all the ab-initio MD simulations the framework structure and the water chains remain stable and show a geometry in reasonable agreement with the experimental findings; moreover, the stability of the one-dimensional ice is independent of the (Si, Al) distribution in the framework. This result is reasonable, with the water chains not being directly connected to the framework oxygen atoms via hydrogen bonds.
3. The simulated vibrational spectrum is in reasonable agreement with the experimental one and is consistent with the presence of the one-dimensional chain of hydrogen-bonded water molecules, in which only one hydrogen per water molecule is involved.
4. The structural properties and the reasons for the formation and stability in bikitaite of this one-dimensional ice deserve further investigation, as being low-dimensional systems they are of great technological interest. Work is in progress in this direction [17].

#### Acknowledgements

We are indebted to Dr Z. Gabelica (Mulhouse, France) for the sample of bikitaite from North Carolina. The authors thank Dr P.G. Fabbri (Centro Interdipartimentale Grandi Strumenti, University of Modena) for the technical assistance during the micro-IR measurements and Professor A. Alberti for the useful discussion. Financial support was provided by Italian MURST (‘Relazione tra struttura e proprietà dei minerali: analisi e applicazioni’, and ‘Sviluppo e applicazioni di metodologie per lo studio di dinamiche molecolari’, cofinanziamento 1997). The authors are indebted to the ‘Centro CNR per lo Studio delle Relazioni tra Struttura e Reattività Chimica’ for grants of computer time.

## References

- [1] G. Bissert, F.N. Liebau, *Jb. Miner. Mh. H* 6 (1986) 241.
- [2] K. Ståhl, Å. Kvik, S. Ghose, *Zeolites* 9 (1989) 303.
- [3] V. Kocman, R. Gait, J. Rucklidge, *Am. Mineral.* 59 (1974) 71.
- [4] C.S. Hurlbut Jr., *Am. Mineral.* 42 (1957) 792.
- [5] P.B. Leavens, C.S. Hurlbut Jr., J.A. Nelen, *Am. Mineral.* 53 (1968) 1202.
- [6] A.C. North, D.C. Phillips, F.S. Mathews, *Acta Crystallogr. Sect. A*: 24 (1968) 351.
- [7] G.M. Sheldrick, SHELX76: Program for Crystal Structure Determination, University of Cambridge, Cambridge, UK, 1976.
- [8] R. Car, M. Parrinello, *Phys. Rev. Lett.* 55 (1985) 2471.
- [9] J. Hutter, P. Ballone, M. Bernasconi, P. Focher, E. Fois, S. Goedecker, M. Parrinello, M. Tuckerman, CPMD Version 3.0, MPI für Festkörperforschung and IBM Research, 1996.
- [10] G. Galli, A. Pasquarello, in: M.P. Allen, D.J. Tildesley (Eds.), *Computer Simulations in Chemical Physics*, Kluwer, Dordrecht, The Netherlands, 1993, p. 261.
- [11] M. Parrinello, *Solid State Commun.* 102 (1997) 107.
- [12] W. Kohn, L.J. Sham, *Phys. Rev. A* 140 (1965) 1133.
- [13] L. Kleinman, D.M. Bylander, *Phys. Rev. Lett.* 48 (1982) 1425.
- [14] N. Troullier, J.L. Martins, *Phys. Rev. B* 43 (1991) 1993.
- [15] A.D. Becke, *J. Chem. Phys.* 96 (1992) 2155.
- [16] J.P. Perdew, *Phys. Rev. B* 33 (1986) 8822.
- [17] E. Fois, G. Tabacchi, S. Quartieri, G. Vezzalini, *J. Chem. Phys.* (1999) in press.
- [18] A. Alberti, G. Gottardi, *Z. Kristallogr.* 184 (1988) 49.
- [19] A. Alberti, in: T. Inui, S. Samba, T. Tatsumi (Eds.), *Chemistry of Microporous Systems*, Kodansha, Tokyo, 1991, pp. 107–121.
- [20] V.M.F. Hammer, E. Libowitzky, G.R. Rossman, *Am. Mineral.* 83 (1998) 569.
- [21] G. Herzberg, *Molecular Spectra and Molecular Structure* vol. II Krieger, Malebar, FL, 1991.
- [22] P.E. Blöchl, *Phys. Rev. B* 50 (1994) 17953.
- [23] V. Wathélet, B. Champagne, D.H. Moseley, J.-M. André, S. Massidda, *Chem. Phys. Lett.* 275 (1997) 506.
- [24] R.B. Ferguson, *Acta Crystallogr. Sect. B*: 30 (1974) 2527.
- [25] S. Merlino, in: D. Olson, A. Bisio (Eds.), *Proceedings of the Sixth International Zeolite Conference* (1983) 747–759.